HortScience 60(9):1494–1502. 2025. https://doi.org/10.21273/HORTSCI18751-25

Declining Phosphorus Availability Increases Sucrose Synthase Activity in 'Beauregard' Sweetpotato Proximal Adventitious Root Tissue Undergoing Storage Root Initiation

Marissa Barbosa, Lisa Arce, Mae Ann Bravo, and Don LaBonte
School of Plant, Environmental, and Soil Sciences, Louisiana State University, 104 Sturgis Hall, Baton Rouge, LA 70803, USA

Shimon Rachmilevitch
French Associates Institute for Agriculture and Biotechnology of Drylands, Jacob Blaustein Institutes for Desert Research, Ben-Gurion University, Sede Boqer Campus, 8499000, Midreshet Ben-Gurion, Israel

Arthur Villordon
Louisiana State University Agricultural Center Sweet Potato Research Station, 130 Sweet Potato Road, Chase, LA 71324, USA

Keywords. *Ipomoea batatas*, lateral roots, root system architecture, sink strength, split-root system

Abstract. **Sucrose synthase (*SuSy*) is recognized as a marker for sink strength in sweetpotato adventitious roots (ARs) undergoing storage root (SR) initiation. However, little is known about specific variables that modulate AR *SuSy* activity. Two studies were performed using a vertical split-root culture system to test the hypothesis from model systems that declining rhizosphere phosphorus (Pi) availability leads to increased carbohydrate accumulation in the root system. In the first study, an experiment was conducted to characterize tissue-specific *SuSy* expression in sweetpotato cv. Beauregard plants subjected to declining Pi treatments during early AR development and SR formation stages. A subsequent experiment was performed to measure *SuSy* activity in the AR proximal tissue (APT) under various Pi availability scenarios. The Pi treatments applied in either compartment was +P/+P, +P/–P, –P/–P, and 0P/0P (+P = Pi sufficient control; 0P = Pi omission; –P = declining Pi). The –P treatment was implemented by reducing Pi by 25%, 50%, 75%, and 100% at 7, 9, 11, and 13 days after planting (DAP), respectively. In the first experiment, APT *SuSy* expression increased from 12 to 15 DAP relative to the root tip and immature leaves, confirming tissue specificity of activity at the onset of SR initiation. In the second experiment, APT *SuSy* activity was higher with –P/–P relative to the control (+P/+P) at 10 to 15 DAP, aligning with prior anatomic evidence regarding the location and timing of SR initiation. Neither the 0P/0P treatment nor the +P/–P treatment elicited a response, suggesting that systemic Pi depletion rate and timing, rather than deficiency alone, are critical for increased sink strength. A second study, which characterized plant height and root system architecture responses, confirmed this presumptive systemic signaling. Taken together, these data support the hypothesis that *SuSy* is a marker for sink strength and that a declining Pi level acts as a developmental cue that signals sweetpotato SR initiation.**

Storage root (SR) initiation is the most economically important physiological process in sweetpotato (*Ipomoea batatas* L.) (Firon et al. 2009). Currently, the only visual marker of SR initiation is the appearance of anomalous cambia around the protoxylem and secondary xylem in stelar tissue (Togari 1950; Wilson and Lowe 1973). Substantial progress has been made in understanding the physiological and molecular mechanisms by which SRs initiate, particularly in terms of the roles of root system architecture (RSA) and starch biosynthesis genes (Firon et al. 2013; Singh et al. 2021; Villordon et al. 2013; Wang et al. 2024). However, current anatomic, physiological, and molecular evidence cannot be reconciled with classic source–sink dynamics—in particular, the identity of variables that increase sink strength in adventitious roots (ARs). Understanding this complex relationship has fundamental and practical implications for improving productivity and economic sustainability in areas where sweetpotatoes are grown. Past evidence has supported the hypothesis that sink strength determines the capacity of ARs to undergo SR initiation (Keutgen et al. 2002; Li and Zhang 2003). Here, we define sink strength as a plant organ's ability to acquire and use photoassimilates effectively, which is determined by both the total biomass of the sink tissue (size and number of tissues) and the intensity of resource uptake (sink activity) (Bihmidine et al. 2013; Chamont 1993). Li and Zhang (2003) correlated sink strength previously with greater sucrose synthase (*SuSy*) activity in sweetpotato SR expressed sequence tags (ESTs) than in non-SR ESTs, and correlated with adenosine diphosphate (ADP)-glucose pyrophosphorylase (AGPase) expression. AGPase catalyzes ADP-glucose formation, the first step in starch synthesis (Hennion et al. 2019). Sucrose is a substrate for starch production and it functions as a signaling molecule that regulates SR development and various metabolic processes (Ravi et al. 2014). Sucrose synthase has been identified previously as a biochemical marker for sink strength in starch-accumulating sink organs such as potato tubers (*Solanum tuberosum*) (Baroja-Fernández et al. 2009; Kaur and Das 2022; Zrenner et al. 1995) and turnip storage roots (*Brassica napus rapifera*) (Gupta et al. 2001), and in rice (*Oryza sativa*) (Counce and Gravois 2006) and maize grains (*Zea mays*) (Li et al. 2023). As starch constitutes the primary carbohydrate reserve of the sweetpotato SR, the genes involved in sucrose-to-starch conversion represent a key regulatory point that could limit SR initiation and overall yield potential. However, the specific signals that regulate *SuSy* activity in sweetpotato ARs remain largely unknown (Villordon and LaBonte 2024).

It is well-documented in model systems that declining rhizosphere phosphorus (Pi) conditions alter plant carbohydrate metabolism, resulting in increased carbon allocation to the root system at the expense of shoot growth (Hermans et al. 2006). In contrast, deficiencies in other nutrients, such as potassium and magnesium, rarely increase belowground biomass despite sugar accumulation in the leaves (Hermans et al. 2006; Vance et al. 2003). Phosphate is one of the least available plant nutrients in soils (Marschner 2011). This nutrient plays a critical role in regulating the expression of multiple genes, including those involved in photosynthesis and carbon metabolism (Lambers 2022). We hypothesize that progressive Pi reduction increases sink strength in ARs, thereby intensifying *SuSy* activity. This study had two objectives. The first was to characterize *SuSy* activity under declining Pi availability in leaf and AR tissues at key stages of AR development. This is to confirm prior findings that anatomic cues associated with the onset of SR initiation are associated with the AR proximal tissue (APT) (2–5 cm from the AR base) with well-developed, first-order lateral roots (LRs) (Villordon et al. 2009a, 2009b, 2012). Second, we wished to characterize tissue-specific APT *SuSy* activity under various Pi availability scenarios. The results of this study have fundamental and applied implications. First, the findings help to bridge significant knowledge gaps in our current understanding of environmental and management cues that trigger the induction of SR formation in sweetpotato

ARs. Second, this knowledge can be harnessed to optimize the management of Pi fertilizers in sweetpotato production.

Materials and Methods

Plant material and growing conditions. In the first study (study 1) two greenhouse experiments were conducted at the Louisiana State University Agricultural Center Sweet Potato Research Station (SPRS) in Chase, LA, USA (lat. 32°6′N, long. 91°42′W) (Table 1). The orange-flesh cultivar Beauregard was used in all experiments. This cultivar was released in 1987 and has been used to characterize the molecular and physiological mechanisms of SR initiation (Rolston et al. 1987; Villordon and LaBonte 2024). The current sweetpotato reference genome was also developed using this cultivar (Fei and Buell 2024). This work used a split-root system (Fig. 1A), which is a relevant tool for addressing the long-distance signaling and remobilization effects of nutrient heterogeneity in the rhizosphere (Flores et al. 2002; Schortemeyer et al. 1993). This growth system enables the separation of local and systemic responses, allowing for a better understanding of their respective molecular mechanisms (Torres et al. 2025). In both experiments, terminal cuttings measuring 25 to 30 cm in length, with six fully expanded leaves and evenly spaced nodes, were obtained from virus-tested plants maintained in the SPRS foundation seed greenhouse (Smith et al. 2009). The experimental setup used 10-cm-diameter polyvinylchloride (PVC) pots (height, 30 cm) with plastic detachable bottoms (Fig. 1A). Each PVC pot had four rows of side drain holes (diameter, 2 mm; spacing, 3 cm apart within rows). These drain holes were added to help reduce the incidence of a perched water table (Bilderback and Fonteno 1987). Washed river sand (diameter, 0.05–0.9 mm) was used as the substrate for all experiments. At planting, vegetative terminal cuttings were positioned to ensure that AR primordia were present in each compartment (Fig. 1B and C). Greenhouse growth conditions were maintained at 29 °C/23 °C (day/night), with a relative humidity of 60% to 80%, and supplemental light-emitting diode lighting to provide a 14 h photoperiod.

Description of experimental treatments. In this work, we simulated the progressive decline in Pi availability in the substrate using the following approach. First, we used half-strength Hoagland's No.1 (Pi = 15 mg·L^{-1}) (+P = Pi sufficient control) solution (Hoagland and Arnon 1950). This nutrient solution concentration has been validated to optimize AR emergence and SR initiation at 5 and 15 d after planting (DAP), respectively, in 'Beauregard' (Villordon and Clark 2018; Villordon et al. 2012, 2013). Second, we reduced available Pi progressively (–P = declining Pi) by 25% (11 mg·L^{-1}), 50% (8 mg·L^{-1}), 75% (4 mg·L^{-1}), and 100% (0 mg·L^{-1}), at 7, 9, 11, and 13 DAP, respectively, corresponding to key AR developmental stages (Villordon et al. 2009a, 2009b). During the establishment phase (1–3 DAP), 50 mL of nutrient solution was applied twice daily to each compartment. This was followed by a 100 mL application to each compartment every other day for the remainder of the experiment. All experiments were arranged in a randomized complete block design, with four replicates per treatment (one pot = one replicate).

The first experiment (Expt. 1; Table 1) was conducted to standardize experimental procedures and to confirm prior findings that anatomic cues associated with the onset of SR initiation is localized in the APT region (2–5 cm from the base), with well-developed lateral branches (Firon et al. 2013; Villordon et al. 2012). Three tissue types were surveyed to assess *SuSy* gene expression: 1) immature leaf tissue, 2) a 2- to 3-cm section of the adventitious root tip (ART), and 3) the APT (Fig. 2). In this experiment, we focused on homogeneous +P/+P (sufficient Pi, 15 mg·L^{-1} in both compartments) and declining –P/–P (declining Pi in both compartments as defined previously).

The second experiment focused on tissue-specific *SuSy* gene expression in the APT region (Expt. 2; Table 1). Four Pi treatments were tested: homogeneous sufficient Pi (+P/+P; 15 mg·L^{-1} in both compartments), homogeneous Pi omission (0P/0P; 0 mg·L^{-1}), homogeneous declining Pi (–P/–P), and heterogeneous Pi (+P/–P). The stepwise reduction in the –P treatment followed the same schedule as described in the first experiment. Based on the findings of the first experiment, which showed no differences between time points 8 and 12 DAP, the sampling time points were reduced to 5, 10, and 15 DAP.

Total RNA extraction and complementary DNA synthesis. Approximately 100 mg of leaf, ART, and APT tissue were collected for RNA extraction. Tissue samples were ground in liquid nitrogen, and total RNA was extracted using the NucleoSpin® RNA Plant (Macherey-Nagel, Bethlehem, PA, USA) according to the manufacturer's instructions, with slight modifications described by Arce et al. (2024). RNA quality and quantity were assessed using a NanoDrop One Spectrophotometer (Thermo Fisher Scientific Inc., Waltham, MA, USA). First-strand complementary DNA (cDNA) synthesis was performed with the iScript cDNA Synthesis Kit (Bio-Rad Laboratories, Hercules, CA, USA) using 1 µg total RNA per 20-µL reaction. All cDNA samples were diluted to 100 ng/µL with nuclease-free water before setting up the quantitative polymerase chain reactions (qPCRs).

Primer design and reverse transcription–qPCR analysis. The *SuSy* gene sequence used in this study was identified in prior work (Arce et al. 2024). The primer pair that was used was forward: 5′-CTGAAATTGAAAAGATGC ACGCT-3′ and reverse: 5′-TTCGTGCACG GTTTGTTTGG-3′.

These primers were designed using Primer 3 Plus (Untergasser et al 2012) and were validated for specificity using the BLAST program. Amplification specificity was tested by melt curve analysis to ensure that only a single melting peak was observed. PCRs and gel electrophoresis were performed to verify the annealing temperature, specificity, and expected product size. qPCR was performed using Bio-Rad Universal SYBR Green Super Mix (Bio-Rad Laboratories) according to the manufacturer's protocol. Each 20-µL reaction contained 2 µL cDNA (100 ng/µL), 0.5 µL of each primer (10 µM), 10 µL master mix, and 7 µL nuclease-free water. Reactions were run on a CFX Duet Real-Time PCR System (Bio-Rad Laboratories) using the following conditions: initial denaturation at 95 °C for 1 min, followed by 40 cycles of denaturation for 15 s at 95 °C, extension for 30 s at 58 °C, and fluorescence plate read at the end of extension step. Melt curve analysis was performed from 65 to 95 °C in increments of 0.5 °C, with a 5-s hold at each step. Negative controls were included with 2 µL nuclease-free water instead of the cDNA template. Each sample was analyzed using four biological and three technical replicates, with sweetpotato *cyclooxygenase* (Park et al. 2012) as the internal reference gene for normalization.

Plant height and RSA measurements. A separate study (study 2) was conducted to generate plants for shoot and root system architecture (RSA) measurements (Table 1). Plant height and RSA measurements were performed at 5, 10, and 15 DAP. For RSA sampling, the detachable plastic bottoms of the pots were removed, the pots were immersed in water, and they were rinsed while holding the stem to prevent AR crossover between compartments. ARs were detached carefully, rinsed with deionized water to

Received for publication 22 May 2025. Accepted for publication 20 Jun 2025.
Published online 5 Aug 2025.
This research was funded by US–Israel Agricultural Research Development Fund Project IS-5512-22: Resilient sweetpotato yield and quality in face of climate change—Root architectural traits for consistent storage root formation under drought. The Louisiana Sweetpotato Advertising and Development Fund also supported portions of this research. This material is based on work that is supported by the National Institute of Food and Agriculture, US Department of Agriculture, Hatch projects.
We thank Cole Gregorie, Adam Easterling, Brandi Juneau, Teresa Hortiguela, Michael Villordon and Mary Ann Munda for the assistance in the conduct of the studies.
M.B. is on study leave from Visayas State University, Visca Baybay City, Leyte, Philippines.
Approved for publication by the Director of the Louisiana Agricultural Experiment Station as manuscript no. 2025-260-40342. Mention of trademark, proprietary product, or method, and vendor does not imply endorsement by the Louisiana State University Agricultural Center nor its approval to the exclusion of other suitable products or vendors.
A.V. is the corresponding author. E-mail: avillordon@agcenter.lsu.edu.

Table 1. Description of greenhouse experiments conducted on sweetpotato cv. Beauregard.

Study	Experiment	Trial	Date planted	Dates harvested	Treatments (Pi levels)[i]	Sampling points (DAP)
1. *SuSy* expression	1. Survey *SuSy* activity in leaf, ART, and APT	A	10 May 2023	16 May 2023	+P/+P and –P/–P	5, 8, 10, 12, and 15
				18 May 2023	+P/+P and –P/–P	5, 8, 10, 12, and 15
				20 May 2023	+P/+P and –P/–P	5, 8, 10, 12, and 15
				22 May 2023	+P/+P and –P/–P	5, 8, 10, 12, and 15
				24 May 2023	+P/+P and –P/–P	5, 8, 10, 12, and 15
	2. Temporal *SuSy* APT activity	A	9 Jun 2023	13 Jun 2023	+P/+P, 0P/0P, –P/–P, +P/–P	5, 10, and 15
				18 Jun 2023	+P/+P, 0P/0P, –P/–P, +P/–P	5, 10, and 15
				23 Jun 2023	+P/+P, 0P/0P, –P/–P, +P/–P	5, 10, and 15
		B	11 Jun 2024	15 Jun 2024	+P/+P, 0P/0P, –P/–P, +P/–P	5, 10, and 15
				20 Jun 2024	+P/+P, 0P/0P, –P/–P, +P/–P	5, 10, and 15
				25 Jun 2024	+P/+P, 0P/0P, –P/–P, +P/–P	5, 10, and 15
2. Biomass measurements	3. Plant height and RSA measurements	A	10 Jun 2023	14 Jun 2023	+P/+P, 0P/0P, –P/–P, +P/–P	5, 10, and 15
				19 Jun 2023	+P/+P, 0P/0P, –P/–P, +P/–P	5, 10, and 15
				24 Jun 2023	+P/+P, 0P/0P, –P/–P, +P/–P	5, 10, and 15
		B	12 Jun 2024	16 Jun 2024	+P/+P, 0P/0P, –P/–P, +P/–P	5, 10, and 15
				21 Jun 2024	+P/+P, 0P/0P, –P/–P, +P/–P	5, 10, and 15
				26 Jun 2024	+P/+P, 0P/0P, –P/–P, +P/–P	5, 10, and 15

[i]Experimental treatments: homogenous high rhizosphere phosphorus (Pi; +P/+P; 15 mg·L^{-1} in both compartments), homogeneous Pi omission (0P/0P; 0 mg·L^{-1}), homogenous declining Pi (–P/–P), and heterogeneous Pi (+P/–P). The –P treatment follows progressive reductions in Pi: 25% (11.3 mg·L^{-1}), 50% (7.5 mg·L^{-1}), 75% (3.75 mg·L^{-1}), and 100% (0 mg·L^{-1}).

ART = adventitious root tip (2–3 cm of the ART); APT = adventitious proximal tissue (2–5 cm from the adventitious root base); DAP = days after planting; RSA = root system architecture; *SuSy* = sucrose synthase.

remove any remaining debris, and then placed in plastic trays filled with water before scanning. During scanning, intact ARs were transferred to a Plexiglas scanner tray (20 × 30 cm) containing water (depth, 3–4 mm). AR samples were staged carefully to minimize overlapping of LRs roots (Fig. 2). Measurements of AR architectural attributes followed the procedures described in prior work (Villordon et al. 2020). Imaging was performed using an Epson Perfection V850 Pro Photo Scanner (Epson Corp., San Jose, CA, USA). Image acquisition parameter was set to high accuracy (600 dpi; image size, ∼18 MB); analysis precision was also set to high. Measured parameters included AR length (in centimeters), AR number, lateral root count (LRC), and lateral root length (LRL). Image J software (Schindelin et al. 2012) was used to measure the length of the main AR (Fig. 2). RhizoVision explorer software (Seethepalli and York 2020) was used to analyze LRC and LRL.

Statistical analysis. Sucrose synthase relative expression was calculated using the $2^{-\Delta\Delta Ct}$ method (Livak and Schmittgen 2001). Standard deviations were calculated from three replicates. Statistical significance was determined using Student's *t* test (one tailed) at $P \leq 0.05$. Root and shoot biomass were analyzed using analysis of variance (ANOVA) using the aov() function in R v. 2024.04.0-735 (R Foundation for Statistical Computing, Vienna, Austria). The ANOVA was followed by Tukey's honestly significant test to identify significant differences using the TukeyHSD() function. Multiple comparisons were done using the HSD.test() functions in R package agricolae v. 1.3-5 (R Foundation for Statistical Computing, Vienna, Austria) (de Mendiburu 2021). There were no significant interaction effects among planting dates for either shoot or root traits; therefore, the data were combined. To assess the RSA response and variability patterns graphically within the RSA data, the R package ggplot2 (Wickham 2016) was used to generate boxplots using R.

Results and Discussion

Shoot and root biomass. Representative plants for each treatment are shown in Fig. 3.

Initially at 5 DAP, Pi-deprived plants (0P/0P) exhibited comparable shoot and root measurements relative to the +P/+P control (Figs. 4 and 5). However, by 10 DAP, 0P/0P reduced shoot growth and suppressed root development significantly, with latter reductions of 26%, 50%, and 37% in in AR number, LRC, and LRL, respectively, relative to +P/+P plants. In contrast, shoot growth with progressive Pi reduction (–P/–P) was comparable to that with +P/+P until 15 DAP. There were no differences in RSA traits across the time points. Heterogeneous Pi treatment (+P/–P) was associated with no changes in shoot or RSA traits relative to +P/+P at any time point. There were no differences in RSA traits between compartments for all treatments.

These responses are consistent with prior evidence in other crop species, in which short-term Pi deprivation does not affect growth immediately as a result of Pi remobilization from stored pools, such as seeds, tubers, or leaves (Barker and Pilbeam 2015; López-Arredondo et al. 2014). However, these internal Pi pools are finite, and external Pi availability is critical for sustained growth (López-Arredondo et al. 2014; Wissuwa 2003). The data also support the role of systemic Pi signaling, in which roots in Pi-rich zones compensate for Pi-deprived regions, enabling sustained growth under spatially variable conditions (Thibaud et al. 2010). Similar compensatory responses have been reported in maize and wheat (*Triticum aestivum*) under heterogeneous Pi supply (Zhu et al. 2005). As a mobile nutrient, Pi can be translocated from Pi-sufficient tissue to demand sites, mitigating localized deficiencies effectively (Barker and Pilbeam 2015; Khan et al. 2023). The shoot and root growth reductions under prolonged Pi deprivation are consistent with previous reports linking Pi deficiency to source–sink disruptions that impair photoassimilate transport and use, consequently limiting sink organ growth (Hermans et al. 2006; Wissuwa 2003). This disruption often leads to feedback inhibition of photosynthesis and a subsequent reduction in overall biomass accumulation (Wissuwa 2003).

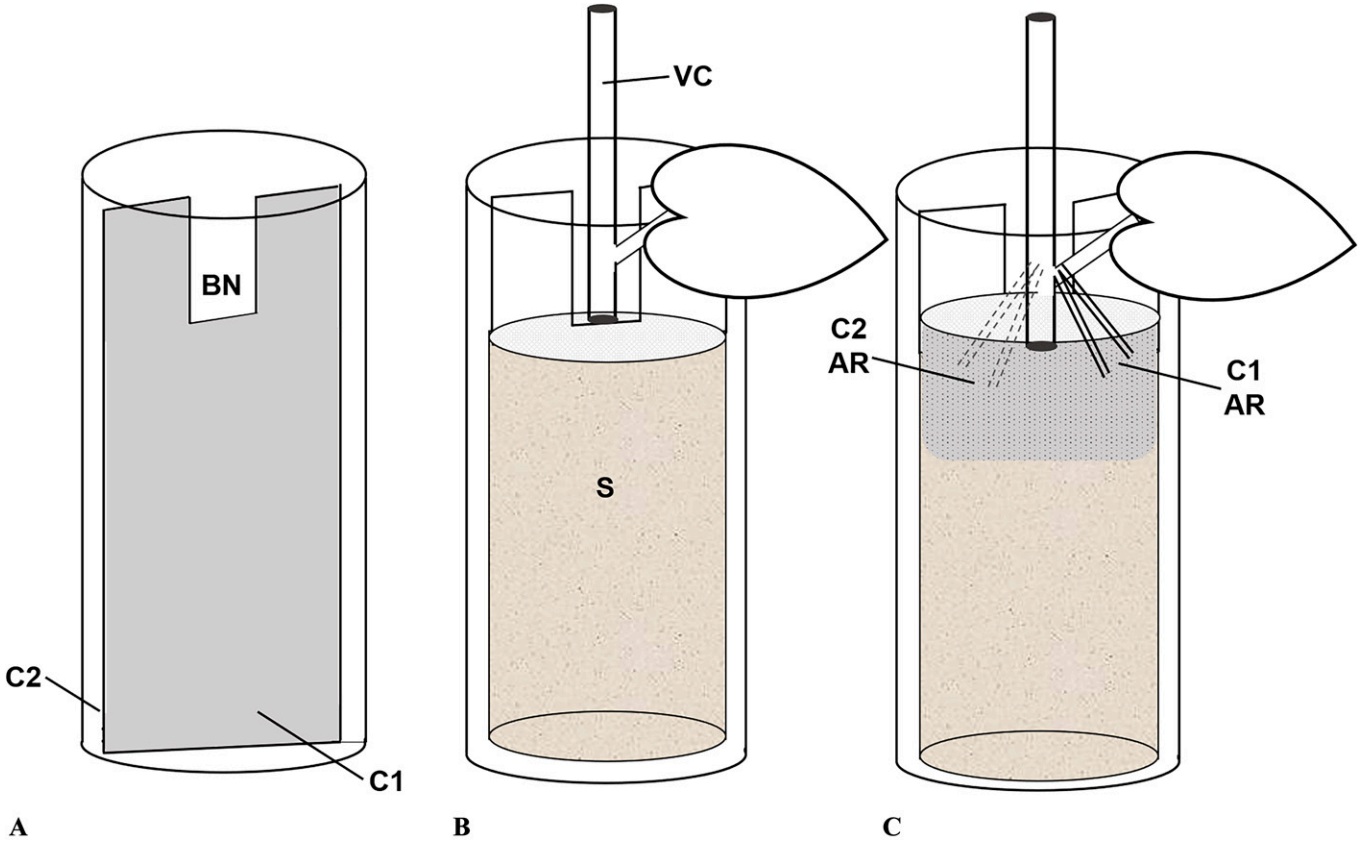

Fig. 1. Schematic of vertical split-root culture system used for simulating local rhizosphere phosphorus variability in sweetpotato cv. Beauregard. An acrylic divider was inserted vertically in each pot to create two compartments: compartment 1 (C1) and compartment 2 (C2) (**A**). The substrate (**S**) was poured into each compartment, initially to the bottom of the notch (BN) (**B**). Vegetative cuttings (VC) were positioned carefully to ensure that adventitious root (AR) primordia were present in each compartment. Additional substrate was added to cover the nodes (**C**).

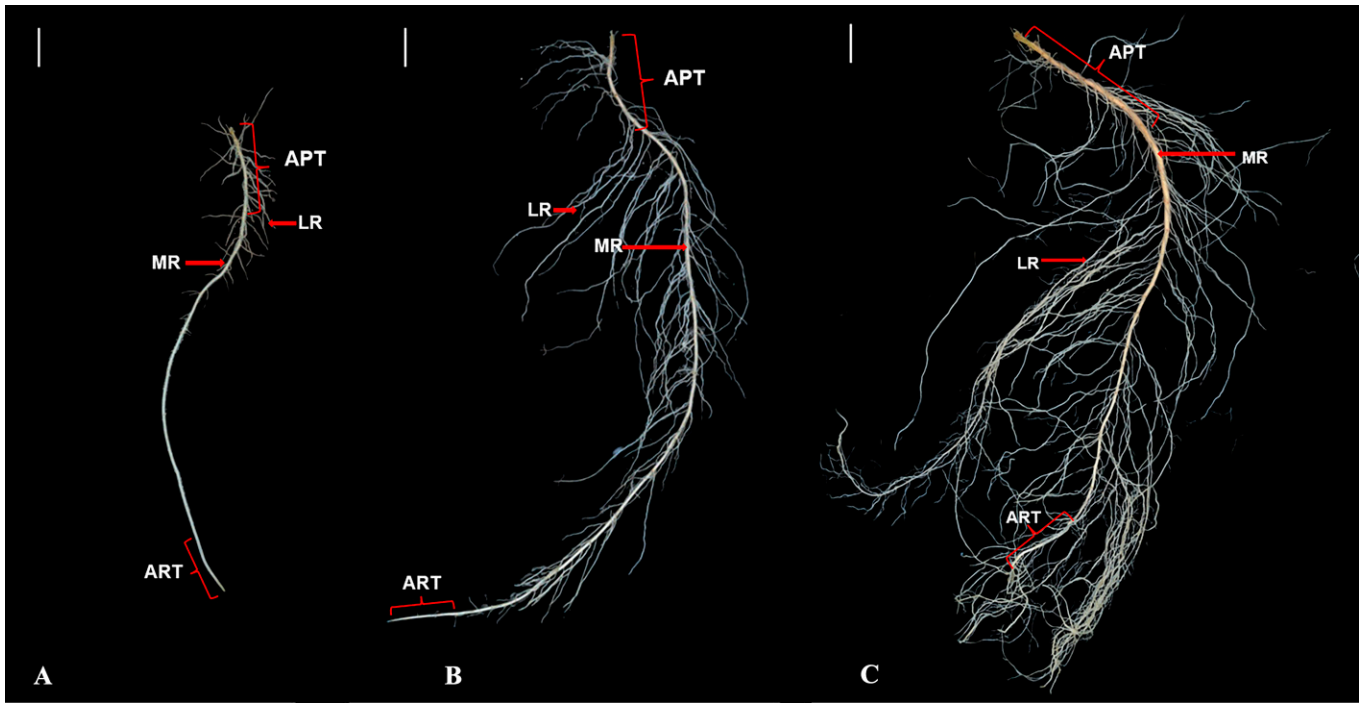

Fig. 2. Scanned adventitious root images of sweetpotato cv. Beauregard sampled at 5 (**A**), 10 (**B**), and 15 (**C**) d after planting (DAP) from control plants (+P/+P) showing the distinct root tissue types used for sucrose synthase gene expression analysis. The adventitious root proximal tissue (APT) at 15 DAP shows localized swelling consistent with storage root formation. Scale bar = 1 cm. ART = adventitious root tip; LR = lateral root; MR = main root.

Fig. 3. Sweetpotato cv. Beauregard plants sampled from the split-root culture system at 5, 10, and 15 d after planting (DAP). Experimental treatments: homogenous sufficient rhizosphere phosphorus (Pi) (+P/+P; 15 mg·L^{-1} in both compartments), homogeneous Pi omission (0P/0P; 0 mg·L^{-1}), homogenous declining Pi (–P/–P), and heterogeneous Pi (+P/–P). The –P treatment follows progressive reductions in Pi: 25% (11.3 mg·L^{-1}), 50% (7.5 mg·L^{-1}), 75% (3.75 mg·L^{-1}), and 100% (0 mg·L^{-1}) applied at 7, 9, 11, and 13 DAP, respectively.

In addition to its effects on photosynthesis, variation in Pi availability modulates RSA traits (Lynch 2011). Under Pi-limiting conditions, plants actively remodel their root systems to enhance nutrient acquisition, a response that includes altering LR development and increasing root hair density (López-Bucio et al. 2003; Lynch 2011; Péret et al. 2011). Consistent with our results, Villordon et al. (2020) demonstrated that Pi availability influences sweetpotato RSA significantly during the critical stage of SR initiation. Specifically, low Pi suppresses AR and LR development, which are key traits closely associated with SR initiation (Villordon et al. 2020).

SuSy *activity increased in APT in response to declining Pi availability.* The findings in Expt. 1 of the study 1 align with prior work that anatomic cues associated with the onset of SR initiation are localized in the APT region (2–5 cm from the base) with well-developed, first-order lateral roots (Firon et al. 2013; Villordon et al. 2012). In the leaf tissue, *SuSy* expression in –P/–P plants did not vary relative to +P/+P plants until 15 DAP (Fig. 6A). In contrast, *SuSy* expression varied temporally in ART and APT regions (Fig. 6B and C). Initially, there were no differences in *SuSy* APT and ART expression in –P/–P relative to +P/+P at establishment (5–8 DAP) (Fig. 6B and C). At 10 DAP, when Pi was reduced by 50%, *SuSy* expression increased in both APT and ART (Fig. 6B and C). This increase coincided with active AR growth and LR development (Fig. 5E–H), suggesting enhanced sink activity, increased carbon requirement, and Pi foraging under nutrient-limited conditions (Li et al. 2024; Stein and Granot 2019). From 12 to 15 DAP, corresponding to the critical stage of SR initiation (Villordon et al. 2020), *SuSy* expression became predominantly localized in APT, with no further induction in the ART. This shift reflects a developmental transition from exploratory root growth toward carbon allocation for storage, consistent with the established role of *SuSy* in sink establishment (Gessler 2021; Li and Zhang 2003).

The APT-specific upregulation of *SuSy* aligns with anatomic cues associated with the transition from ARs to storage roots (Firon et al. 2013; Villordon et al. 2012). This transition involves the formation of anomalous cambia around the protoxylem and secondary xylem, facilitating secondary thickening and starch accumulation (Togari 1950; Wilson and Lowe 1973). More important, such cambial activity is localized within the proximal 2 to 3 cm of ARs, with optimal LR development (Firon et al. 2013; Villordon et al. 2012). Our

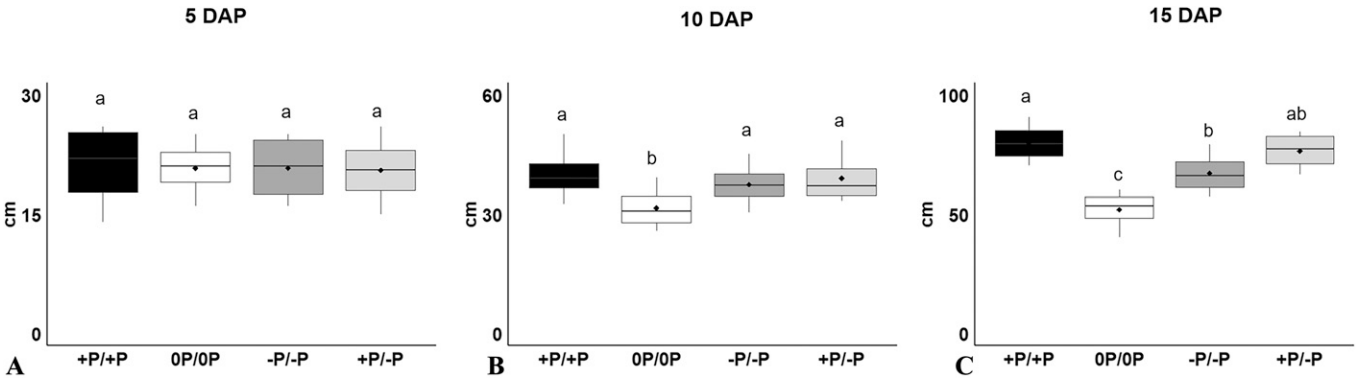

Fig. 4. Sweetpotato cv. Beauregard plant height response to varying rhizosphere phosphorus (Pi) availability at 5 (**A**), 10 (**B**), and 15 (**C**) days after planting (DAP). Experimental treatments: homogenous sufficient Pi (+P/+P; 15 mg·L^{-1} in both compartments), homogeneous Pi omission (0P/0P; 0 mg·L^{-1}), homogenous declining Pi (–P/–P), and heterogeneous Pi (+P/–P). The –P treatment follows progressive reductions in Pi: 25% (11.3 mg·L^{-1}), 50% (7.5 mg·L^{-1}), 75% (3.75 mg·L^{-1}), and 100% (0 mg·L^{-1}) applied at 7, 9, 11, and 13 DAP, respectively. Statistical differences are indicated by lowercase letters (Tukey's honestly significant difference test, $P \leq 0.05$). Boxes represent the interquartile range (IQR), or middle 50%, of values for each feature. Black diamonds represent mean values. Bold horizontal lines indicate median values. Upper boxplot whiskers represent the last data point within the range of the 75% quantile + 1.5 IQR; lower boxplot whiskers represent the last data point within the range of the 25% quantile – 1.5 IQR. Black circles represent outliers (values smaller or larger than the median ± 1.5 times the IQR).

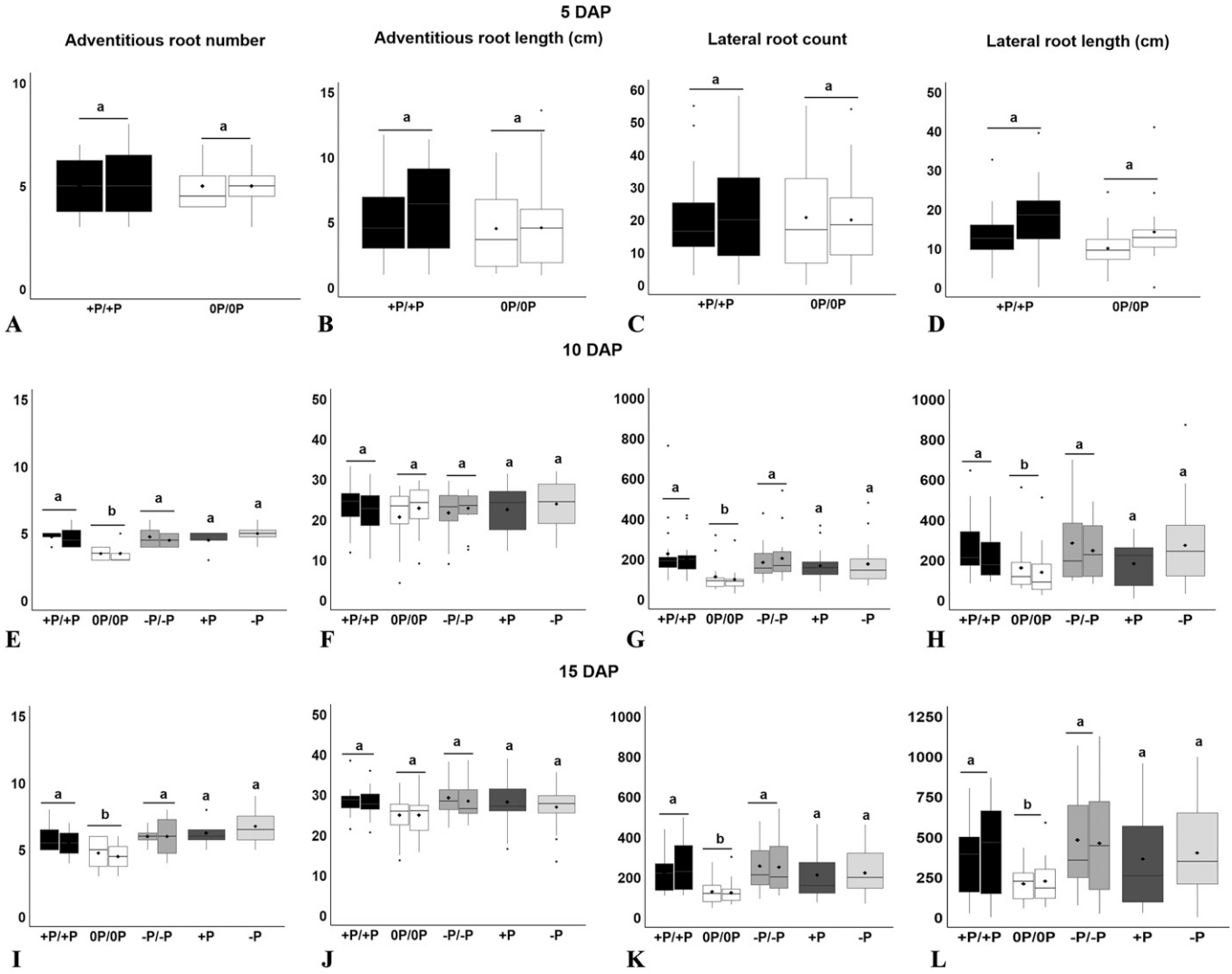

Fig. 5. Boxplots of root architectural attributes in sweetpotato cv. Beauregard in response to varying rhizosphere phosphorus (Pi) availability at 5 (**A–D**), 10 (**E–H**), and 15 (**I–L**) d after planting (DAP) under the split-root system. Experimental treatments: homogenous sufficient Pi (+P/+P; 15 mg·L^{-1} in both compartments), homogeneous Pi omission (0P/0P; 0 mg·L^{-1}), homogenous declining Pi (–P/–P), and heterogeneous Pi (+P/–P). The –P treatment follows progressive reductions in Pi: 25% (11.3 mg·L^{-1}), 50% (7.5 mg·L^{-1}), 75% (3.75 mg·L^{-1}), and 100% (0 mg·L^{-1}) applied at 7, 9, 11, and 13 DAP, respectively. The average values of two compartments for +P/+P, –P/–P, and 0P/0P were calculated to compare among treatments. Statistical differences are indicated by lowercase letters (Tukey's honestly significant difference test, $P \leq 0.05$). Boxes represent the interquartile range (IQR), or middle 50% of values for each feature. Black diamonds represent mean values. Bold horizontal lines indicate median values. Upper boxplot whiskers represent the last data point within the range of the 75% quantile + 1.5 IQR; lower boxplot whiskers represent the last data point within the range of the 25% quantile – 1.5 IQR. Black circles represent outliers (values smaller or larger than the median ± 1.5 times the IQR).

results corroborate this spatial specificity, with APT exhibiting increased *SuSy* activity relative to ART, which supports the hypothesized role of *SuSy* as a marker for enhanced sink strength during SR initiation (Li and Zhang 2003). Previous studies support these observations. For example, Firon et al. (2013) defined and used this AR region for transcriptomic analysis and measured gene expression of genes involved in sucrose and starch metabolism during SR initiation. Furthermore, Singh et al. (2021) showed the proliferation of starch-accumulating parenchymal cells associated with bulking in the APT region. Similar patterns have been reported in cassava (*Manihot esculenta*), in which elevated *SuSy* expression in basal root tissues correlates with early starch deposition (Huang et al. 2021).

Temporal SuSy *activity in the APT. SuSy* expression in Expt. 2 of study 1 was constant across compartments with homogeneous Pi levels (+P/+P, 0P/0P, and –P/–P) at all time points (Supplemental Fig. 1). Based on these results, RNA samples from both compartments were pooled for analysis. Declining Pi availability (–P/–P) increased *SuSy* activity relative to the control (+P/+P) at 10 and 15 DAP across 2 years (Fig. 7B, C, E, and F). In contrast, homogeneous 0P/0P was not associated with increased *SuSy* activity across time points and both years (Fig. 7A–F). In the heterogeneous Pi treatment (+P/–P), *SuSy* expression initially did not vary across compartments at 10 DAP (Fig. 7B and E). However, at 15 DAP, *SuSy* activity increased in both compartments.

Prior work has linked sucrose signaling in sweetpotato SR initiation, but scant information is available about what modulates sink strength (Ahn et al. 2010; Li and Zhang 2003; Zhang et al. 2017). Our findings demonstrate that declining Pi availability increases sink strength in ARs undergoing SR initiation, as evidenced by increased *SuSy* activity. The increased *SuSy* activity in ARs undergoing SR initiation is consistent with findings reported by Li and Zhang (2003). These findings are consistent with increased *SuSy* activity in turnip SRs during the early, rapid sink filling phase, accompanied by a concomitant reduction in leaf *SuSy* activity (Gupta et al. 2001). A similar pattern of increased *SuSy* activity at the early stage of potato tuber initiation has also been documented previously (Kaur and Das 2022). Our results are consistent with available evidence that supports the hypothesis that *SuSy* is a molecular marker for sink strength in starch-accumulating sink organs [reviewed in Fernie et al. (2020)].

Our results corroborate findings in the model plant *Arabidopsis*, in which sugars are

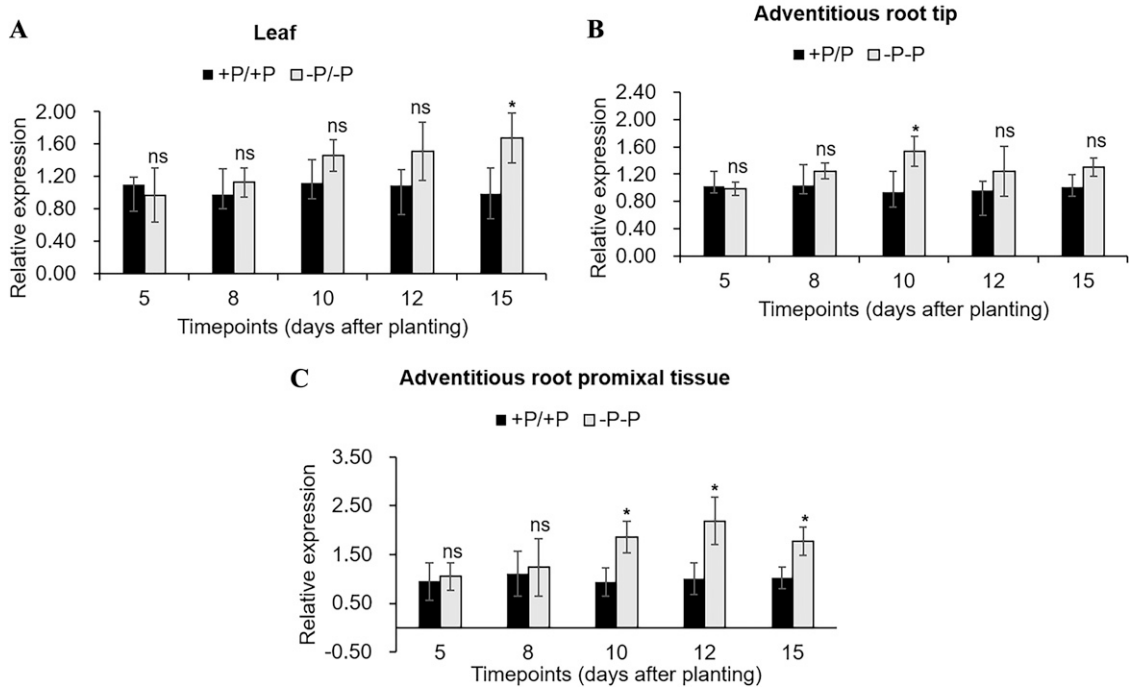

Fig. 6. Sucrose synthase expression in sweetpotato cv. Beauregard leaf (**A**), root tip (**B**), and proximal zone (**C**) of the adventitious roots at 5, 8, 10, 12, and 15 d after planting using a split-root culture system. Experimental treatments: homogenous sufficient Pi (+P/+P; 15 mg·L^{-1} in both compartments), homogeneous Pi omission (0P/0P; 0 mg·L^{-1}), homogenous declining Pi (–P/–P), and heterogeneous Pi (+P/–P). The –P treatment follows progressive reductions in Pi: 25% (11.3 mg·L^{-1}), 50% (7.5 mg·L^{-1}), 75% (3.75 mg·L^{-1}), and 100% (0 mg·L^{-1}) applied at 7, 9, 11, and 13 DAP, respectively. Transcript levels are expressed relative to +P plants and normalized using the sweetpotato *cyclooxygenase* reference gene. Data represent the mean of three biological replicates. ns, * Nonsignificant and significant at $P \leq 0.05$ (Student's *t* test), respectively. Error bars represent standard deviation.

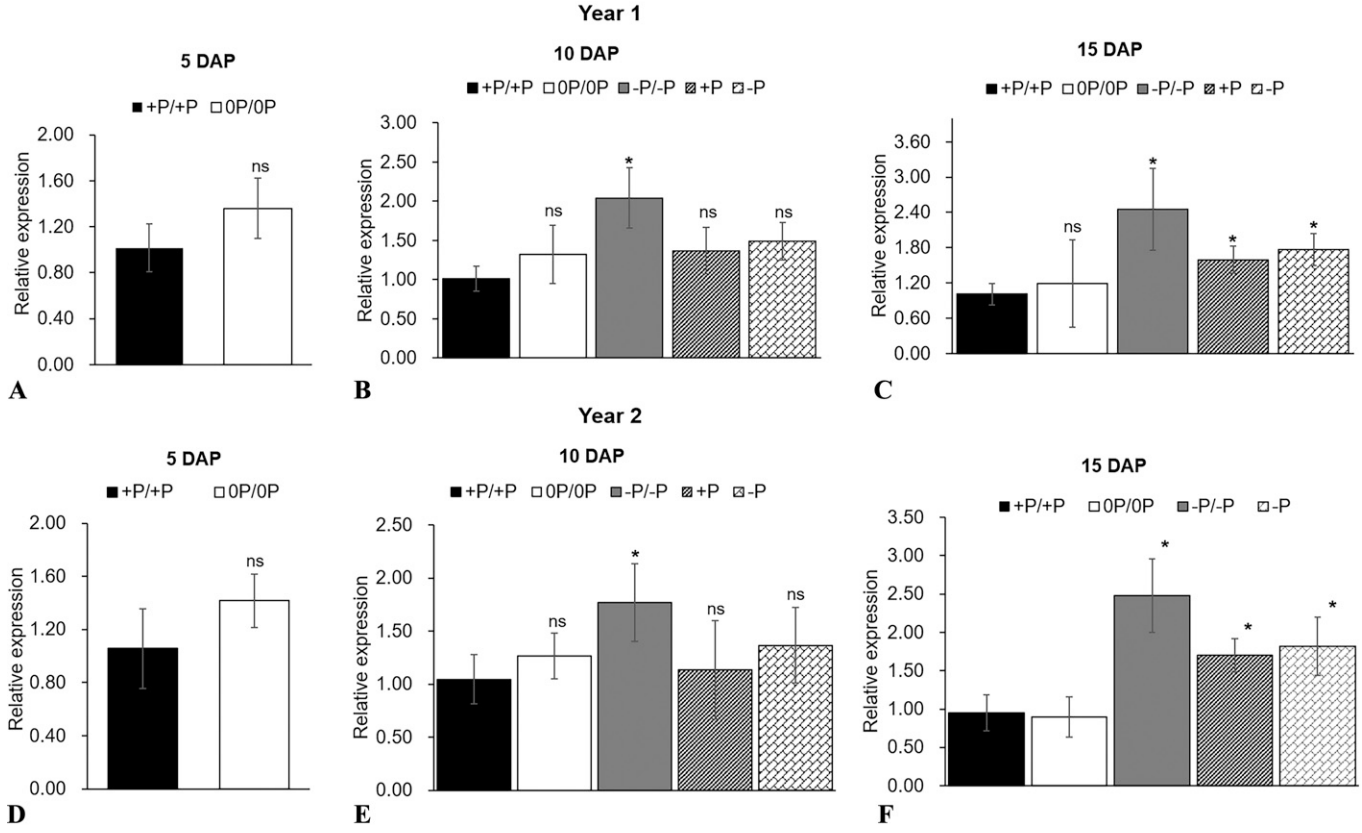

Fig. 7. Sucrose synthase expression in sweetpotato cv. Beauregard adventitious root proximal tissue with varying phosphorus levels at 5, 10, and 15 d after planting (DAP) in year 1 (**A**–**C**) and year 2 (**D**–**F**) using a split-root culture system. Experimental treatments: homogenous sufficient Pi (+P/+P; 15 mg·L^{-1} in both compartments), homogeneous Pi omission (0P/0P; 0 mg·L^{-1}), homogenous declining Pi (–P/–P), and heterogeneous Pi (+P/–P). The –P treatment follows progressive reductions in Pi: 25% (11.3 mg·L^{-1}), 50% (7.5 mg·L^{-1}), 75% (3.75 mg·L^{-1}), and 100% (0 mg·L^{-1}) applied at 7, 9, 11, and 13 DAP, respectively. Transcript levels are expressed relative to +P/+P plants (homogenous supplementation of 15 mg·L^{-1} Pi), and normalized using the sweetpotato *cyclooxygenase* reference gene. Data represent the mean of three biological replicates. ns, * Nonsignificant and significant at $P \leq 0.05$ (Student's *t* test), respectively. Error bars represent standard deviation.

redistributed preferentially to the root system in response to reduced Pi availability (Hammond and White 2008; Hermans et al. 2006). In addition, reduced Pi triggers the production of intracellular phosphatases and nucleases that facilitate Pi remobilization from internal pools, further supporting sustained metabolism in developing sinks (Hammond and White 2011; Müller et al. 2007; Soumya et al. 2022). These processes are believed to be coordinated with sugar signaling pathways. In this case, the increased root sucrose levels also regulate genes encoding RNases, phosphatases, and the phosphate starvation response (PSR) transcriptional cascade to remobilize internal Pi or alter root biochemistry and morphology for efficient Pi uptake (Fang et al. 2009; Karthikeyan et al. 2007; Ruan 2014; Yoon et al. 2021). In sweetpotato, Arce et al. (2024) reported that low Pi activates PSR transporters *IbPHT1;4* and *IbPHT1;5* in 'Bayou Belle', but not in 'Evangeline' or 'Orleans'. This is consistent with the hypothesis that variation in *SuSy* activity may also reflect cultivar-specific differences in SR initiation and timing.

Our work used a split-root system. In the past, this system has been used to investigate the possible presence of local and systemic responses to the variation of Pi availability in root systems (Flores et al. 2002; Torres et al. 2025; Schortemeyer et al. 1993). Our morphological and molecular data using 'Beauregard' do not appear to show responses to local Pi availability. However, novel molecular data support the hypothesis of cultivar-specific Pi sensitivity (Arce et al. 2024). Previous data also show RSA variation among cultivars subjected to reduced Pi availability (Villordon et al. 2018, 2020). We hypothesize that cultivars adapted to low Pi availability may respond differently to heterogeneous Pi levels.

The results of our study have fundamental and applied implications. First, the findings help to bridge significant knowledge gaps in our current understanding of environmental and management cues that trigger the induction of SR initiation in sweetpotato ARs. Follow-up studies can focus on cultivar-specific sensitivity to Pi depletion. Accounting for this genotypic variability is essential, as specific cultivars may require a higher initial Pi rate, whereas others may respond optimally to sustained, moderate Pi levels. Second, the potential role of other nutrients cannot be ruled out. Third, the findings can be leveraged to optimize the management of Pi fertilizers in sweetpotato production. For example, our results underscore the importance of applying the optimum Pi fertilizer rate. Applying excessive amounts may potentially delay the induction of storage root formation in putatively low-Pi-requiring cultivars. Taken together, these findings underscore the potential for considering soil Pi levels and cultivar for developing site-specific management approaches for improved sweetpotato production efficiency.

Conclusion

Our study presents the first evidence of a direct link between phosphorus availability and *SuSy* activity, leading to increased sink strength in sweetpotato. Our findings support the hypothesis that declining Pi availability serves as a key developmental cue, enhancing *SuSy* gene expression and increasing sink strength in sweetpotato ARs. This response coincides with the early stages of SR initiation, suggesting that Pi may function as a metabolic switch regulating the transition of ARs into SRs. Future research should aim to characterize cultivar-specific Pi thresholds and sensitivities that trigger increased *SuSy* activity and SR initiation.

References Cited

Ahn YO, Kim SH, Kim CY, Lee JS, Kwak SS, Lee HS. 2010. Exogenous sucrose utilization and starch biosynthesis among sweetpotato cultivars. Carbohydr Res. 345(1):55–60. https://doi.org/10.1016/j.carres.2009.08.025.

Arce LI, Labonte D, Villordon A, Gregorie JC. 2024. Differential expression of phosphate starvation-responsive genes among sweetpotato cultivars during establishment and onset of storage root formation. J Am Soc Hortic Sci. 149(6):311–319. https://doi.org/10.21273/JASHS05433-24.

Barker AV, Pilbeam DJ. 2015. Handbook of Plant Nutrition (2nd ed). CRC Press, Boca Raton, FL, USA. https://doi.org/10.1201/b18458.

Baroja-Fernández E, Muñoz FJ, Montero M, Etxeberria E, Sesma MT, Ovecka M, Bahaji A, Ezquer I, Li J, Prat S, Pozueta-Romero J. 2009. Enhancing sucrose synthase activity in transgenic potato (*Solanum tuberosum* L.) tubers results in increased levels of starch, ADPglucose and UDPglucose and total yield. Plant Cell Physiol. 50(9):1651–1662. https://doi.org/10.1093/pcp/pcp108.

Bihmidine S, Hunter CT, Johns CE, Koch KE, Braun DM. 2013. Regulation of assimilate import into sink organs: Update on molecular drivers of sink strength. Front Plant Sci. 4:177. https://doi.org/10.3389/fpls.2013.00177.

Bilderback TE, Fonteno WC. 1987. Effects of container geometry and media physical properties on air and water volumes in containers. J Environ Hortic. 5(4):180–182. https://doi.org/10.24266/0738-2898-5.4.180.

Chamont S. 1993. Sink strength: The key for plant yield modeling. Plant Cell Environ. 16(9):1033–1034. https://doi.org/10.1111/j.1365-3040.1996.tb02056.x.

Counce PA, Gravois KA. 2006. Sucrose synthase activity as a potential indicator of high rice grain yield. Crop Sci. 46(4):1501–1507. https://doi.org/10.2135/cropsci2005.0240.

de Mendiburu F. 2021. agricolae tutorial (version 1.3-5). Universidad Nacional Agraria, La Molina, Peru.

Fang Z, Shao C, Meng Y, Wu P, Chen M. 2009. Phosphate signaling in *Arabidopsis* and *Oryza sativa*. Plant Sci. 176(2):170–180. https://doi.org/10.1016/j.plantsci.2008.09.007.

Fei Z, Buell CR. 2024. Ipomoea batatas 'Beauregard' genome assembly v4 and annotation. University of Georgia, Athens, GA, USA. https://sweetpotato.uga.edu/sweetgains_Beauregard_v4_asm_anno.shtml. [accessed 20 Nov 2024].

Fernie AR, Bachem CWB, Helariutta Y, Neuhaus HE, Prat S, Ruan Y-L, Stitt M, Sweetlove LJ, Tegeder M, Wahl V, Sonnewald S, Sonnewald U. 2020. Synchronization of developmental, molecular and metabolic aspects of source–sink interactions. Nat Plants. 6(2):55–66. https://doi.org/10.1038/s41477-020-0590-x.

Firon N, LaBonte D, Villordon A, Kfir Y, Solis J, Lapis E, Perlman T, Doron-Faigenboim A, Hetzroni A, Althan L, Nadir L. 2013. Transcriptional profiling of sweetpotato (*Ipomoea batatas*) roots indicates down-regulation of lignin biosynthesis and up-regulation of starch biosynthesis at an early stage of storage root formation. BMC Genomics. 14(1):460. https://doi.org/10.1186/1471-2164-14-460.

Firon N, LaBonte D, Villordon A, McGregor C, Kfir Y, Pressman E. 2009. Botany and physiology: storage root formation and development, p 13–26. In: Loebenstein G, Thottappilly G (eds). The sweetpotato. Springer, Dordrecht, Netherlands. https://doi.org/10.1007/978-1-4020-9475-0_3.

Flores P, Angeles Botella M, Martínez V, Cerdá A. 2002. Response to salinity of tomato seedlings with a split-root system: Nitrate uptake and reduction. J Plant Nutr. 25(1):177–187. https://doi.org/10.1081/PLN-100108789.

Gessler A. 2021. Sucrose synthase: An enzyme with a central role in the source–sink coordination and carbon flow in trees. New Phytol. 229(1):8–10. https://doi.org/10.1111/nph.16998.

Gupta AK, Singh J, Kaur N. 2001. Sink development, sucrose metabolising enzymes and carbohydrate status in turnip (*Brassica rapa* L.). Acta Physiol Plant. 23(1):31–36. https://doi.org/10.1007/s11738-001-0019-8.

Hammond JP, White PJ. 2008. Sucrose transport in the phloem: integrating root responses to phosphorus starvation. J Exp Bot. 59(1):93–109. http://doi:10.1093/jxb/erm221.

Hammond JP, White PJ. 2011. Sugar signaling in root responses to low phosphorus availability. Plant Physiol. 156(3):1033–1040. https://doi.org/10.1104/pp.111.175380.

Hennion N, Durand M, Vriet C, Doidy J, Maurousset L, Lemoine R, Pourtau N. 2019. Sugars en route to the roots: Transport, metabolism and storage within plant roots and towards microorganisms of the rhizosphere. Physiol Plant. 165(1):44–57. https://doi.org/10.1111/ppl.12751.

Hermans C, Hammond JP, White PJ, Verbruggen N. 2006. How do plants respond to nutrient shortage by biomass allocation? Trends Plant Sci. 11(12):610–617. https://doi.org/10.1016/j.tplants.2006.10.007.

Hoagland DR, Arnon DI. 1950. The water–culture method for growing plants without soil (2nd ed). California Agricultural Exp Stn Circ 347.

Huang T, Luo X, Fan Z, Yang Y, Wan W. 2021. Genome-wide identification and analysis of the sucrose synthase gene family in cassava (*Manihot esculenta* Crantz). Gene. 769:145191. https://doi.org/10.1016/j.gene.2020.145191.

Karthikeyan AS, Varadarajan DK, Jain A, Held MA, Carpita NC, Raghothama KG. 2007. Phosphate starvation responses are mediated by sugar signaling in *Arabidopsis*. Planta. 225(4):907–918. https://doi.org/10.1007/s00425-006-0408-8.

Kaur G, Das N. 2022. An isoform of sucrose synthase involved in sink strength of potato (*Solanum tuberosum* L.): Molecular cloning, sequence analyses, 3-D structure, crucial motifs and expression. South Afr J Bot. 149:446–457. https://doi.org/10.1016/j.sajb.2022.06.032.

Keutgen N, Mukminah F, Roeb GW. 2002. Sink strength and photosynthetic capacity influence tuber development in sweet potato. J Hortic Sci Biotech. 77(1):106–115. https://doi.org/10.1080/14620316.2002.11511465.

Khan F, Siddique AB, Shabala S, Zhou M, Zhao C. 2023. Phosphorus plays key roles in regulating plants' physiological responses to abiotic

stresses. Plants (Basel). 12(15):2861. https://doi.org/10.3390/plants12152861.
Lambers H. 2022. Phosphorus acquisition and utilization in plants. Annu Rev Plant Biol. 73(73):17–42. https://doi.org/10.1146/annurev-arplant-102720-125738.
Li J, Hu Y, Hu J, Xie Q, Chen X, Qi X. 2024. Sucrose synthase: An enzyme with multiple roles in plant physiology. J Plant Physiol. 303:154352. https://doi.org/10.1016/j.jplph.2024.154352.
Li P, Ma H, Xiao N, Zhang Y, Xu T, Xia T. 2023. Overexpression of the *ZmSUS1* gene alters the content and composition of endosperm starch in maize (*Zea mays* L.). Planta. 257(5):97. https://doi.org/10.1007/s00425-023-04133-z.
Li XQ, Zhang D. 2003. Gene expression activity and pathway selection for sucrose metabolism in developing storage root of sweet potato. Plant Cell Physiol. 44(6):630–636. https://doi.org/10.1093/pcp/pcg080.
Livak KJ, Schmittgen TD. 2001. Analysis of relative gene expression data using real-time quantitative PCR and the 2(-Delta Delta C(T))method. Methods. 25(4):402–408. https://doi.org/10.1006/meth.2001.1262.
López-Arredondo DL, Leyva-González MA, González-Morales SI, Herrera-Estrella L, López-Hernández LF. 2014. Phosphorus acquisition strategies in plants: Understanding the physiological and molecular mechanisms. Plant Physiol. 166(3):657–666. https://doi.org/10.1104/pp.114.248674.
López-Bucio J, Cruz-Ramírez A, Herrera-Estrella L. 2003. The role of nutrient availability in regulating root architecture. Curr Opin Plant Biol. 6(3):280–287. https://doi.org/10.1016/s1369-5266(03)00035-9.
Lynch JP. 2011. Root phenes for enhanced soil exploration and phosphorus acquisition: Tools for future crops. Plant Physiol. 156(3):1041–1049. https://doi.org/10.1104/pp.111.175414.
Marschner H. 2012. Marschner's Mineral Nutrition of Higher Plants, 3rd ed. Academic Press, San Diego, CA, USA.
Müller R, Morant M, Jarmer H, Nilsson L, Nielsen TH. 2007. Genome-wide analysis of the *Arabidopsis* leaf transcriptome reveals interaction of phosphate and sugar metabolism. Plant Physiol. 143(1):156–171. https://doi.org/10.1104/pp.106.090167.
Park SC, Kim YH, Ji CY, Park S, Jeong JC, Lee HS, Kwak SS. 2012. Stable internal reference genes for the normalization of real-time PCR in different sweetpotato cultivars subjected to abiotic stress conditions. PLoS One. 7(12):e51502. https://doi.org/10.1371/journal.pone.0051502.
Péret B, Clément M, Nussaume L, Desnos T. 2011. Root developmental adaptation to phosphate starvation: Better safe than sorry. Trends Plant Sci. 16(8):442–450. https://doi.org/10.1016/j.tplants.2011.05.006.
Ravi V, Chakrabarti SK, Makeshkumar T, Saravanan R. 2014. Molecular regulation of storage root formation and development in sweet potato, p 157–208. In: Janick J (ed). Horticultural Reviews (vol 42). Wiley-Blackwell. Hoboken, NJ, USA. https://doi.org/10.1002/9781118916827.ch03.
Rolston LH, Clark CA, Cannon JM, Randle WM, Riley EG, Wilson PW, Robbins ML. 1987. 'Beauregard' sweet potato. HortScience. 22(6):1338–1339. https://doi.org/10.21273/HORTSCI.22.6.1338.
Ruan YL. 2014. Sucrose metabolism: Gateway to diverse carbon use and sugar signaling. Annu Rev Plant Biol. 65(1):33–67. https://doi.org/10.1146/annurev-arplant-050213-040251.
Schindelin J, Arganda-Carreras I, Frise E, Kaynig V, Longair M, Pietzsch T, Preibisch S, Rueden C, Saalfeld S, Schmid B, Tinevez JY, White DJ, Hartenstein V, Eliceiri K, Tomancak P, Cardona A. 2012. Fiji: An open-source platform for biological-image analysis. Nat Methods. 9(7):676–682. https://doi.org/10.1038/nmeth.2019.
Schortemeyer M, Feil B, Stamp P. 1993. Root morphology and nitrogen uptake of maize simultaneously supplied with ammonium and nitrate in a split-root system. Ann Bot. 72(2):107–115. https://doi.org/10.1006/anbo.1993.1087.
Seethepalli A, York LM. 2020. RhizoVision Explorer: Interactive software for generalized root image analysis designed for everyone (version 2.0.2). Zenodo Geneva, Switzerland. https://doi.org/10.5281/zenodo.4095629.
Singh V, Zemach H, Shabtai S, Aloni R, Yang J, Zhang P, Sergeeva L, Ligterink W, Firon N. 2021. Proximal and distal parts of sweetpotato adventitious roots display differences in root architecture, lignin, and starch metabolism and their developmental fates. Front Plant Sci. 11:609923. https://doi.org/10.3389/fpls.2020.609923.
Smith TP, Stoddard S, Shankle M, Schultheis J. 2009. Sweetpotato production in the United States, p 287–323. In: Loebenstein G, Thottappilly G (eds). The sweetpotato. Springer, Dordrecht, Netherlands.
Soumya PR, Vengavasi K, Pandey R. 2022. Adaptive strategies of plants to conserve internal phosphorus under P deficient condition to improve P utilization efficiency. Physiol Mol Biol Plants. 28(11–12):1981–1993. https://doi.org/10.1007/s12298-022-01255-8.
Stein O, Granot D. 2019. An overview of sucrose synthases in plants. Front Plant Sci. 10:95. https://doi.org/10.3389/fpls.2019.00095.
Thibaud M-C, Arrighi J-F, Bayle V, Chiarenza S, Creff A, Bustos R, Paz-Ares J, Poirier Y, Nussaume L. 2010. Dissection of local and systemic transcriptional responses to phosphate starvation in *Arabidopsis*. Plant J. 64(5):775–789. https://doi.org/10.1111/j.1365-313X.2010.04375.x.
Togari Y. 1950. A study of tuberous root initiation in sweetpotato. Tokyo Nat Agric Exp Stn Bull 68. [in Japanese with English summary].
Torres LF, de Andrade SA, Mazzafera P. 2025. Phosphorus uptake in eucalypt plants under split root system. Trop Plant Biol. 18:40. https://doi.org/10.1007/s12042-025-09410-7.
Untergasser A, Cutcutache I, Koressaar T, Ye J, Faircloth BC, Remm M, Rozen SG. 2012. Primer3-new capabilities and interfaces. Nucleic Acids Res. 40(15):e115. https://doi.org/10.1093/nar/gks596.
Vance CP, Uhde-Stone C, Allan DL. 2003. Phosphorus acquisition and use: Critical adaptations by plants for securing a nonrenewable resource. New Phytol. 157(3):423–447. https://doi.org/10.1046/j.1469-8137.2003.00695.x.
Villordon A, Gregorie JC, LaBonte D, Khan A, Selvaraj M. 2018. Variation in 'Bayou Belle' and 'Beauregard' Sweetpotato Root Length in Response to Experimental Phosphorus Deficiency and Compacted Layer Treatments. HortScience. 53(10):1534–1540. https://doi.org/10.21273/HORTSCI13305-18.
Villordon A, Gregorie JC, LaBonte D. 2020. Variation in phosphorus availability, root architecture attributes, and onset of storage root formation among sweetpotato cultivars. HortScience. 55(12):1903–1911. https://doi.org/10.21273/HORTSCI-15358-20.
Villordon A, LaBonte D. 2024. Advances in our understanding of the genetic regulation of storage root formation and growth, p 111–122. In: Yencho GC, Olukolu BA, Isobe S (eds). The Sweetpotato genome. Springer International Publishing, Cham, Switzerland.
Villordon A, LaBonte D, Firon N. 2009a. Development of a simple thermal time method for describing the onset of morpho-anatomic features related to sweetpotato storage root formation. Sci Hortic. 121(3):374–377. https://doi.org/10.1016/j.scienta.2009.02.013.
Villordon AQ, LaBonte DR, Firon N, Kfir Y, Pressman E, Schwartz A. 2009b. Characterization of adventitious root development in sweetpotato. HortScience. 44(3):651–655. https://doi.org/10.21273/HORTSCI.44.3.651.
Villordon A, LaBonte D, Firon N, Carey E. 2013. Variation in nitrogen rate and local availability alter root architecture attributes at the onset of storage root initiation in 'Beauregard' sweetpotato. HortScience. 48(6):808–815. https://doi.org/10.21273/HORTSCI.48.6.808.
Villordon A, LaBonte D, Solis J, Firon N. 2012. Characterization of lateral root development at the onset of storage root initiation in 'Beauregard' sweetpotato adventitious roots. HortScience. 47(7):961–968. https://doi.org/10.21273/HORTSCI.47.7.961.
Wang D, Li C, Liu H, Song W, Shi C, Li Q. 2024. Sweetpotato sucrose transporter *IbSUT1* alters storage roots formation by regulating sucrose transport and lignin biosynthesis. Plant J. 120(3):950–965. https://doi.org/10.1111/tpj.17029.
Wickham H. 2016. ggplot2: Elegant Graphics for Data Analysis. Springer-Verlag, New York, USA.
Wilson LA, Lowe SB. 1973. The anatomy of the root system in West Indian sweet potato (*Ipomoea batatas* L.) cultivars. Ann Bot. 37(3):633–643. https://doi.org/10.1093/oxfordjournals.aob.a084729.
Wissuwa M. 2003. How do plants achieve tolerance to phosphorus deficiency? Small causes with big effects. Plant Physiol. 133(4):1947–1958. https://doi.org/10.1104/pp.103.029306.
Yoon J, Cho L, Tun H, Jeon WJ, An G. 2021. Sucrose signaling in higher plants. Plant Sci. 302:110703. https://doi.org/10.1016/j.plantsci.2020.110703.
Zhang K, Wu Z, Tang D, Luo K, Lu H, Liu Y, Dong J, Wang X, Lv C, Wang J, Lu K. 2017. Comparative transcriptome analysis reveals critical function of sucrose metabolism related-enzymes in starch accumulation in the storage root of sweet potato. Front Plant Sci. 8:914. https://doi.org/10.3389/fpls.2017.00914.
Zhu J, Kaeppler SM, Lynch JP. 2005. Topsoil foraging and phosphorus acquisition efficiency in maize (*Zea mays*). Funct Plant Biol. 32(8):749–762. https://doi.org/10.1071/FP05005.
Zrenner R, Salanoubat M, Willmitzer L, Sonnewald U. 1995. Evidence of the crucial role of sucrose synthase for sink strength using transgenic potato plants (*Solanum tuberosum* L.). Plant J. 7(1):97–107. https://doi.org/10.1046/j.1365-313x.1995.07010097.x.